JMEPEG (2012) 21:2074–2079
DOI: 10.1007/s11665-012-0135-1

1059-9495/$19.00

Pack Cementation Coatings for High-Temperature Oxidation Resistance of AISI 304 Stainless Steel

Morteza Zandrahimi, Javad Vatandoost, and Hadi Ebrahimifar

(Submitted March 5, 2011; in revised form January 6, 2012)

Aluminum and titanium are deposited on the surface of steel by the pack cementation method to improve its hot-corrosion and high-temperature oxidation resistance. In this research, coatings of aluminum and titanium and a two-step coating of aluminum and titanium were applied on an AISI 304 stainless steel substrate. The coating layers were examined by carrying out scanning electron microscopy (SEM) and x-ray diffraction (XRD). The SEM results showed that the aluminized coating consisted of two layers with a thickness of 450 µm each, the titanized coating consisted of two layers with a thickness of 100 µm each, and the two-step coatings of Al and Ti consisted of three layers with a thickness of 200 µm each. The XRD investigation of the coatings showed that the aluminized coating consisted of Al_2O_3, $AlCr_2$, FeAl, and Fe_3Al phases; the titanized layers contained TiO_2, Ni_3Ti, FeNi, and Fe_2TiO_5 phases; and the two-step coating contained AlNi, Ti_3Al, and FeAl phases. The uncoated and coated specimens were subjected to isothermal oxidation at 1050 °C for 100 h. The oxidation results revealed that the application of a coating layer increased the oxidation resistance of the coated AISI 304 samples as opposed to the uncoated ones.

Keywords AISI 304 stainless steel, aluminizing, oxidation, titanizing, two-step deposition of Al and Ti

1. Introduction

Stainless steels are employed in numerous applications because of their good performance in different environments and their relatively low price. They are used in industrial processes related to carbochemistry, petrochemical and power plants, gasification systems, combustion, aerospace, etc. (Ref 1-3). During service at high temperatures, ferritic, martensitic, and austenitic steels constitute a protective chromia oxide scale on their surface which stays homogenous, continuous, and well adherent to the metallic substrate, which forms a diffusion barrier against environmental attack. This surface layer will be destabilized above 1000 °C and will not protect the substrate (Ref 4).

One approach for overcoming these problems is through the application of a protective coating on stainless steels. High-temperature-resistant coatings, like diffusional coatings, are expected to protect the substrate from evaporation of chromium at high temperatures. Aluminide coatings are beneficial for high-temperature materials because of their practical advantages in comparison with the coatings which are employed at low temperatures (Ref 5-8). Also titanium coatings and titanium aluminides are being considered as promising materials for high-temperature applications.

Morteza Zandrahimi, Javad Vatandoost, and **Hadi Ebrahimifar,** Department of Metallurgy and Materials Science, Faculty of Engineering, Shahid Bahonar University of Kerman, Jomhoori Eslami Blvd., Kerman, Iran. Contact e-mail: m.zandrahimi@mail.uk.ac.ir.

Over the various techniques that have been developed to apply protective diffusional coatings on stainless steels, pack cementation is one of the most effective techniques for oxidation resistance purposes. Pack cementation is basically an in-situ, self-generated chemical vapour deposition (CVD) process (Ref 9). This process is a versatile process and normally used to deposit diffusion coating on the various alloys. This generic technology enables depositing single or multiple elemental coatings on steels or other alloys (Ref 5-7).

Pack aluminizing has been widely applied to steels and super alloys to improve their hot-temperature oxidation resistance (Ref 9). Pack cementation coatings, especially aluminide and titanide coatings, produce intermetallic compounds (FeAl, Fe_3Al, and Ti_3Al), which have been an important topic for research and development over the last few decades because of their high melting points, low densities, and excellent oxidation resistance at high temperatures (Ref 10-14).

The reason for investigating three types of pack cementation coatings particularly aluminide and titanium-aluminides are because of the high temperature oxidation resistance of these coatings. Aluminum, titanium, and aluminum-titanium coatings were used on other alloys but not on AISI 304. Therefore, in order to investigate the effect of these three types of coatings on the high-temperature oxidation resistance of AISI 304 and to evaluate which coating is the most effective, this research was carried out.

The present study evaluates the microstructure and oxidation behavior of aluminized, titanized, and two-step aluminized-titanized AISI 304 stainless steel.

2. Experimental Procedure

In this research, AISI 304 stainless steel with a thickness of 2 mm was used as substrate material. Sheets of steels were

annealed at 950 ± 15 °C for 1 h to relieve internal stress. The chemical composition (wt.%) of steel is given in Table 1. Specimens were cut and sized to approximately 10 mm × 10 mm, and the surfaces of the samples were ground and polished up to 0.25 lm diamond finish. The samples were subsequently degreased and ultrasonically cleaned in ethanol for 5 min, dried, and weighed before coating.

The pack powder mixtures used for the deposition of Al and Ti were prepared by weighing out and mixing appropriate amounts of the powders of Al and Al_2O_3 or Ti and Al_2O_3, respectively; NH_4Cl was used as an activator. In this study, three types of pack cementation processes were carried out: aluminization, titanization, and two-step aluminization-titanization (including simple aluminization and titanization). The pack components, process parameters, and types of treated specimens are shown in Table 2. The average powder particle size was less than 75 lm. The optimum pack composition is shown in Table 1. The powder mixture was composed of Al_2O_3 82 wt.% (inert filler), Al 15 wt.%, and NH_4Cl_3 wt.% (activator). The packs were prepared by filling the powder mixture around the substrates in a cylindrical alumina crucible measuring 35 mm in diameter and 20 mm in length. The crucible was then sealed with an alumina lid using high-temperature cement. The cement seal was cured for 24 h at room temperature and further cured at an oven temperature of about 100 °C for 1 h. The pack was then loaded into a horizontal tubular furnace circulated with argon, and the temperature of the furnace was raised and held for different periods of time. After the pack cementation treatment, the crucible was cooled down to room temperature in an argon flux. The specimen was removed from the pack, ultrasonically cleaned in ethanol, and weighed. The surfaces and cross sections of the specimens were analyzed to determine the morphology, thickness, and composition of the coatings.

The cross sections of the coated samples were examined using optical microscopy and SEM equipped with an energy-dispersive x-ray spectroscopy (EDS) analyzer. Diffusion profiles of Al and Ti across the coating cross sections were derived by EDS. X-ray diffraction (XRD) was used to identify the phases formed in the coatings using an XRD (Phillips X'Pert) with Cu-K_α radiation operating at a sampling rate of 0.6°(2θ) per minute. To investigate the isothermal oxidation behavior of the as-coated samples, an oxidation resistance test was carried out at 1050 °C in air in an electrical furnace. During oxidation at 1050 °C, the samples were weighed at room temperature several times on an electronic balance with a sensitivity of 0.1 mg.

Table 1 Chemical composition of AISI 430 stainless steel

Element	C	Cr	Si	Mn	P	Ni	Fe
Concentration, wt.%	0.08	19.1	1	1.6	0.045	8.2	69.97

Table 2 Powder composition, annealing temperature and time of pack cementation process

Number	Powder composition	Temp., °C	Time, h
1	Al 10% + NH_4Cl 5% + Al_2O_3 85%	1050	6
2	Ti 15% + NH_4Cl 5% + Al_2O_3 80%	1000	5
3	Al 10% + NH_4Cl 5% + Al_2O_3 85% Then Ti 10% + NH_4Cl 5% + Al_2O_3 85%	1000 900	6 5

3. Results and Discussion

3.1 Aluminizing

An SEM image of the specimen coated with aluminum is shown in Fig. 1(a). The elemental distribution across the coating layer was determined using an EDS analyzer, which is shown in Fig. 1(b). The coating consists of an interfacial zone and an outer zone. The outer zone is approximately 200 μm thick; and the interfacial zone, which is about approximately 200 μm thick, is lighter in shade than the outer zone (Fig. 1a). The concentration profiles measured by the EDS analyzer revealed a two-layer phase structure across the thickness of the coating layer (Fig. 1b). The Al concentration varied from

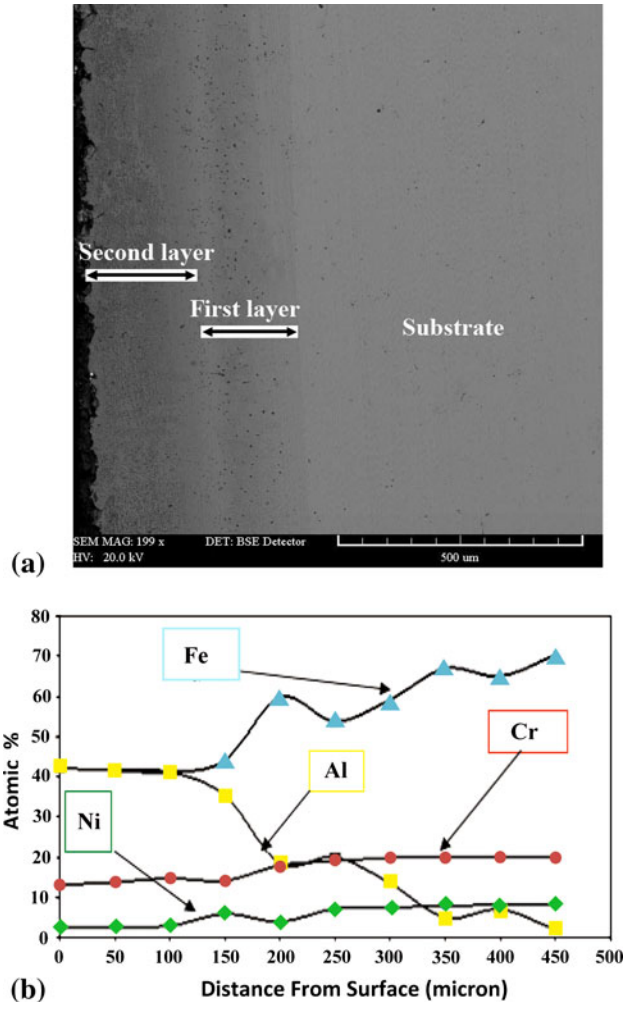

Fig. 1 SEM cross-sectional micrograph of aluminized sample (a) and EDS results showing the concentration variations of Fe, Cr, Ni, and Al elements near the surface of the aluminized 304 stainless steel (b)

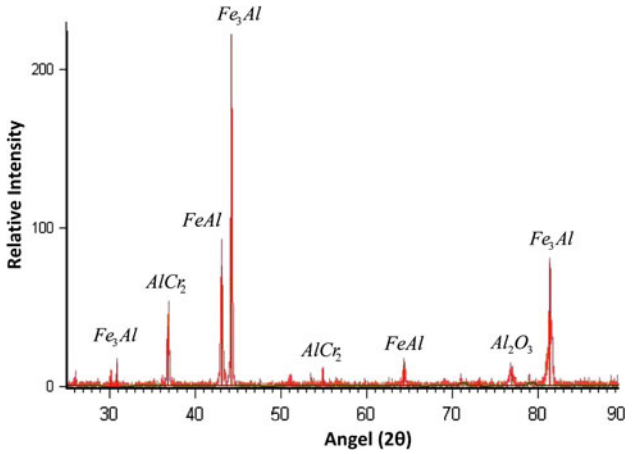

Fig. 2 XRD analysis of aluminized sample

approximately 42 at.% just below the surface to approximately 18 at.% at a depth of about 250 nm from the surface of the coating. However, below this depth, the Al concentration showed a sudden decrease to about 5 at.%. The elemental distribution across the coating layer indicates that the Al content in the interfacial zone was less than that in the outer zone (Fig. 1b). Thus, it is concluded that two types of phases were formed. The upper regions near the surface of the samples mainly consisted of FeAl.

Figure 2 shows an XRD diffractogram of the as-coated surface. As shown in the figure, the surface layer contained mostly Fe_3Al and FeAl phases, and $AlCr_2$ and Al_2O_3 phases were also detected. However, the diffraction peaks of these phases were weak, suggesting that the quantities of these phases in the surface layer were very small. Thus, it appears that the deposited aluminum was present mostly in the solid solution of Fe_3Al.

Intermetallics such as Fe_3Al and FeAl exhibit remarkable resistance to high-temperature oxidation and corrosion. In the case of 304 stainless steel, a pack with low Al content induced the formation of intermetallic phases, such as FeAl, which are instrumental in facilitating corrosion protection. Therefore, the survivals of the FeAl and Fe_3Al phases prove that an outward diffusion of the substrate elements occurred in the aluminizing process.

3.2 Titanizing

Figure 3 shows the cross-sectional SEM image (Fig. 3a) and concentration profiles of Ti and the major elements (Fig. 3b) in the coating layer; the concentration profiles were measured by EDS following a one-step pack cementation process at 1000 °C for 5 h. The element concentration profiles confirm that Ti was deposited on the coated sample from the vapour phase, resulting in the formation of a Ti-rich uniform coating layer. The formation of two distinct layers was observed in the microstructures of the coated samples. The concentration profiles indicate that Ti was present mostly in the outer layer of the coating, which is about 38% below the surface of the coating. The concentration of Ti in the inner layer of the coating gradually decreases toward the substrate. The outer layer is approximately 18 μm thick, and the inner layer has a thickness of 90 μm.

Figure 4 shows the XRD plot of the surface of the coated sample, which confirms the presence of Ni_3Ti, TiO_2, FeNi, and Fe_2TiO_3 phases in the coating layer. The entrapment of oxygen

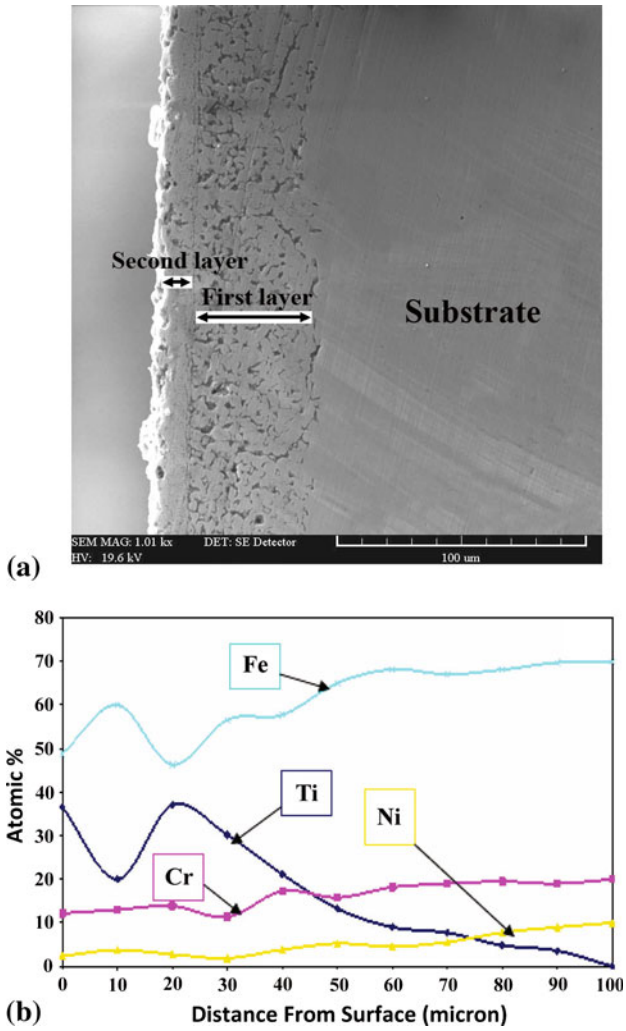

Fig. 3 SEM cross-sectional micrograph of titanized sample (a) and EDS results showing the concentration variations of Fe, Cr, Ni, and Ti elements near the surface of the aluminized 304 stainless steel (b)

in the pack led to the oxidation of Ti and the formation of TiO_2 and Fe_2TiO_3 phases in the coating layer. TiO_2 exhibits good oxidation resistance and can improve the high-temperature performance of coated AISI 304 stainless steel. Furthermore, titanium nitrides like Ni_3Ti are considered to serve as protective layers on metal surface for improving the wear, corrosion, and oxidation resistance of metal.

3.3 Two-Step Aluminizing-Titanizing

Figure 5 shows a cross-sectional SEM image (Fig. 5a) and concentration profiles of the codeposited Al and Ti (Fig. 5b) as well as the coating layer, as measured by EDS. The first step of aluminizing was carried out at a temperature of 1000 °C, and the second step, titanizing, at a temperature of 900 °C. As shown in the SEM image, the coating consisted of three uniform layers with thicknesses of 60, 70, and 50 μm. The 60-μm thick outer layer contained mostly Al and Ti with very little Fe, Cr, or Ni, suggesting that this layer is a Ti-aluminide layer. On the other hand, the middle layer contained Al, Fe, and small amounts of Ti, Cr, and Ni, indicating that this layer is essentially an aluminide layer. The inner layer contained mostly Fe and Al with a small amount of Cr; the presence of these

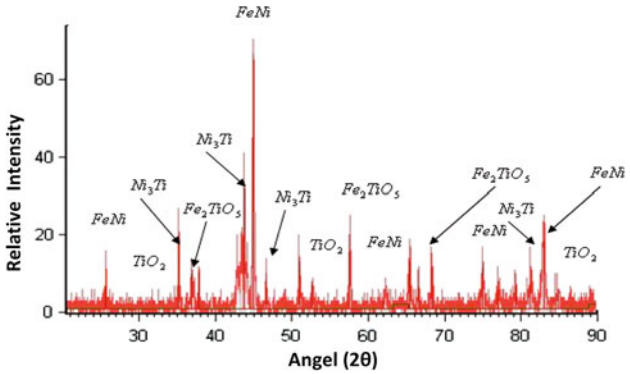

Fig. 4 XRD analysis of titanized sample

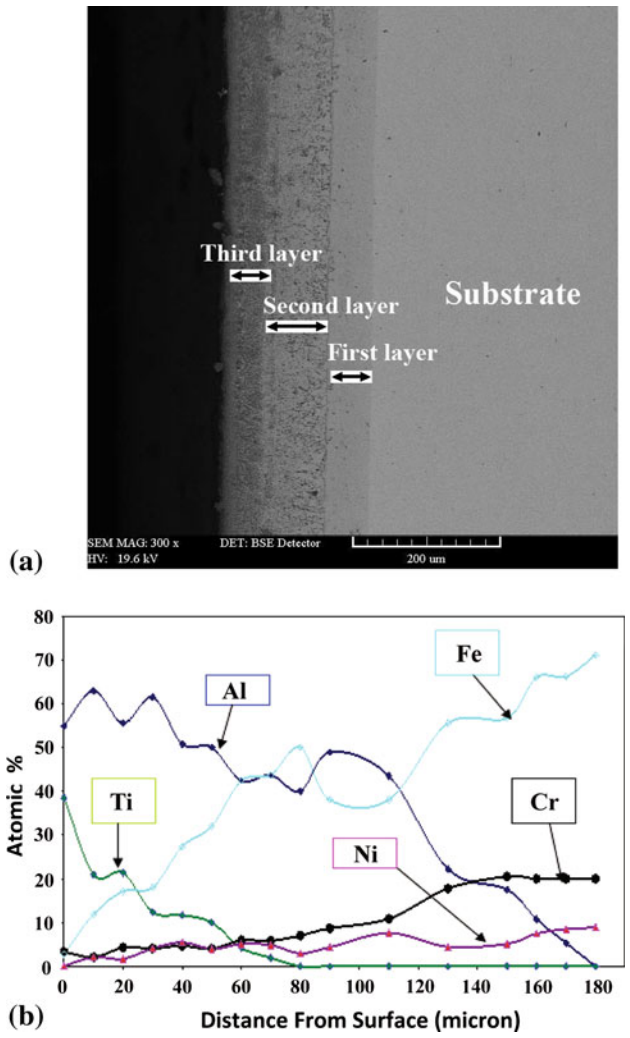

Fig. 5 SEM cross-sectional micrograph of Al-Ti coating (a) and EDS results showing the concentration variations of Fe, Cr, Ni, Al, and Ti elements near the surface of the aluminized 304 stainless steel (b)

elements was determined from the Al and Ti concentration profiles. It can be seen that the Al concentration varies gradually across the depth of this diffusion zone up to the substrate. The XRD results of the two-step coatings are shown in Fig. 6. The figure shows that the coatings are mainly

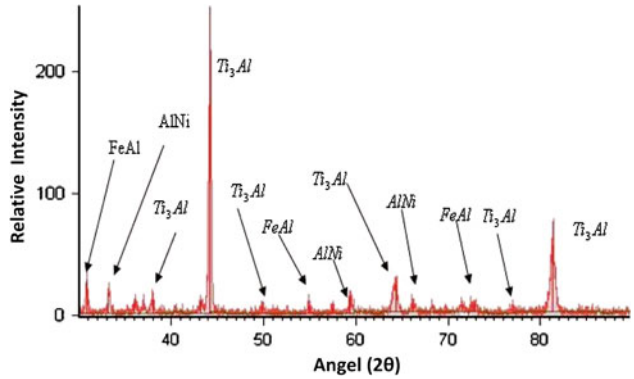

Fig. 6 XRD analysis of Al-Ti coating

composed of the Ti_3Al phase and small peaks of the AlNi and FeAl phases.

The main components of titanium aluminides thermodynamically induce the formation of very stable oxides under oxidizing conditions at high temperatures. Further, the formation of a protective alumina scale is necessary to provide long-term oxidation resistance to substrates at elevated temperatures. On the other hand, titanium oxides form very rapidly and raise the upper limit of temperature resistance of a substrate to approximately 550 °C. According to thermodynamic calculations, titanium aluminides containing more than 48-50 at.% of aluminum are anticipated to form slowly growing alumina scales (Ref 15).

On the basis of a binary phase diagram of Al-Ti alloys (Ref 16), the intermetallic compound Ti_3Al is formed at 23 wt.% of aluminum.

At a reaction temperature of 950 °C, aluminum particles transitioned from a solid to a liquid state. A high aluminum concentration on the surface of molten aluminum droplets and the Al-Ti binary phase diagram indicate the formation of Ti_3Al. At the reaction temperature, Ti_3Al was formed on the surface of the molten aluminum droplets, which resulted in the formation of a solid outer shell and the separation of the shell from the core, thereby avoiding further reaction of Ti_3Al with $TiCl_4$. Thermodynamic calculations on the $TiCl_4$-Ti_3Al system revealed that at lower temperatures, the TiAl phase is more stable than the Ti_3Al phase. The absence of other Al-Ti intermetallic compounds such as AlTi in the second layer of the coating can be attributed to kinetic problems and the absence of thermodynamic equilibrium.

3.4 Oxidation Behavior

Isothermal oxidation kinetics of the uncoated and coated AISI 304 specimens are shown in Fig. 7. At 1050 °C, the isothermal oxidation behavior of all the specimens followed the parabolic rate law.

In all the cases, the weight of the specimens increased parabolically with the isothermal oxidation time, thereby satisfying the parabolic kinetic law (this indicates that oxide scales that formed on the specimen surfaces can act as a diffusion barrier), as given by Eq 1:

$$\left(\frac{\Delta W}{A}\right)^2 = k_p t \qquad \text{(Eq 1)}$$

where ΔW is the sample weight gain, A is the sample surface area, k_p is the parabolic rate constant, and t is the oxidation time.

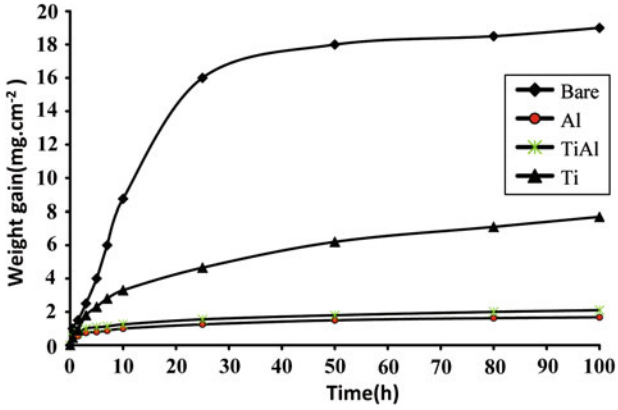

Fig. 7 Weight change curves in air at 1050 °C for Al, Ti, and Al-Ti coatings and substrate

The initial oxidation rate was found to be remarkably high for the uncoated sample; this can be attributed to the bare substrate of the uncoated samples, which oxidized freely.

The oxidation curve of the pack cementation coatings shows two stages. The first stage shows a rapid increase in oxidation owing to nucleation and the formation of an oxide layer. However, the oxide layer thickened as oxidation proceeded, and therefore, the oxidation rate reduced in this stage, resulting in a parabolic shape of the oxidation curve. As seen in this figure, all the three coatings increased the oxidation resistance of the steel.

The aluminized specimens exhibited excellent high-temperature oxidation resistance at 1050 °C. The oxidation resistances of the aluminized and aluminized-titanized specimens were found to be higher than that of the uncoated specimens.

After 100 h of isothermal oxidation, a black oxide scale, which spalled from the sample surface in some areas, was formed on the uncoated sample. The oxide scales on the titanized sample also spalled in some regions of the sample surface. On the other hand, the aluminized and codeposited samples exhibited good resistance against spallation and cracking after 100 h of isothermal oxidation. Oxide scale spallation commonly occurs in materials exposed to high temperatures. The stress produced during oxidation can delaminate the oxide from the metal because oxide scales and the coating below the scales invariably have different thermal expansion coefficients.

The above mentioned results indicate that the present coatings formed a protective oxide layer on the specimens. The parabolic rate constants of the specimens with aluminized coatings were lower than those with titanized coatings. The parabolic rate constants of the bare substrate, aluminized specimen, titanized specimen, and aluminized-titanized specimen were 9.86×10^{-12}, 8.33×10^{-14}, 1.31×10^{-12}, and 9.16×10^{-14} g^2 cm^{-4} s^{-1}, respectively. Evidently, the oxidation resistance of the aluminized coatings was higher than that of the titanized coatings. At 1050 °C, the specimens showed apparent weight loss after 10 h. This weight loss of the specimens imply that at an air temperature greater than 1000 °C, the specimens were no longer oxidation resistant because of the evaporation of chromium oxide from the specimens. The simple Ti-coated specimens showed considerable weight loss because of the spallation of oxide scales after the initial oxidation.

XRD analyses revealed that a large amount of Cr_2O_3 was formed on the surface of the uncoated specimens because of selective oxidation in the initial stage. However, solid Cr_2O_3 can convert into volatile CrO_3 that evaporates during oxidation at 1000 °C (Ref 2, 17, 18), and thus, it cannot impede the diffusion of oxygen ions into the substrate.

Furthermore, iron oxides (Fe_2O_3 and Fe_3O_4) were observed on the surfaces of the uncoated specimens. Consequently, the absence of a protective layer on the surfaces of the uncoated specimens can be attributed to the oxidation of Fe.

Thus, the oxidation resistance of the coated substrates increased because of the presence of the coating elements, intermetallic compounds, or oxides, which restricted the rapid diffusion of oxygen through the coating layer, thus impeding the oxidation of the substrate.

Intermetallic compounds increase the oxidation resistance of materials especially in the regions of grain boundaries or grains. In fact, the increase in the concentration of solute atoms in grain boundaries leads to the build-up of solute atoms, thereby counteracting diffusion through the grain boundaries (Ref 19). Apparently, Al-Fe intermetallics are more effective than Al-Ti intermetallics in reducing diffusion rate. Several other factors can explain the high oxidation resistance of aluminized specimens compared with the aluminized-titanized and titanized specimens. In the case of coatings that contained more than one layer, surface diffusion through each layer would be prevented by the outer layer. In fact, with the creation of complicated diffusion paths, the movement of chromium cations and oxygen anions would be largely restricted. Another factor that can explain the high oxidation resistance of aluminized specimens is the presence of voids and pores. The number of voids and pores in the alumina coating was lower than that in the alumina-titania and titania coating. Even though the alumina-titania coating contained three diffusion layers, the existence of voids and pores in the coating facilitated easy diffusion through these defects. The titania coating exhibited the lowest oxidation resistance among all the coatings. The thermal expansion coefficient of Ti-Al and Ti oxides differed from that of the substrate, resulting in spallation and cracks in the substrate. Spalled scales create diffusion paths for cations and anions to move freely, and therefore, through an easy migration of ions, the oxide layer in the substrate grew at a high rate.

In general, the application of alumina, alumina-titania, and titania coatings increased the high-temperature oxidation resistance of AISI 304 stainless steel.

4. Conclusions

1. Phases of Fe_3Al, FeAl, Al_2O_3, and $AlCr_2$ were observed in an aluminized coating consisting of two thick layers without any pores or voids; this indicated the occurrence of an activity that produced a low amount of char and was accompanied by the outward diffusion of elements from the substrate.
2. In the titanizing process, the Ti coating was found to consist of two layers that contained Fe_2TiO_5, TiO_2, Ni_3Ti, and FeNi phases.
3. The two-step coating of Al and Ti mainly consisted of aluminides of Fe, Ti, and Ni intermetallics.
4. The diffusion lengths for Al and Ti in the two-step coating were 180 and 80 μm, respectively. This difference in the diffusion length could be attributed to the lower atomic radius of Al in comparison to Ti.

5. Alumina, alumina-titania, and titania coatings increased the oxidation resistance of AISI 304 stainless steel by impeding the outward diffusion of Cr cations and inward diffusion of oxygen anions.

References

1. F. Riffard, H. Buscail, E. Caudron, R. Cueff, C. Issartel, and S. Perrier, The Influence of Implanted Yttrium on the Cyclic Oxidation Behaviour of 304 Stainless Steel, *Appl. Surf. Sci.*, 2006, **252**(10), p 3697–3706
2. F.J. Pérez, M. Jcristóbal, M.P. Hierro, and F. Pedraza, The Influence of Implanted Silicon on the Cyclic Oxidation Behavior of Two Different Stainless Steels, *Surf. Coat. Technol.*, 1999, **120–121**, p 442–447
3. D. Laverde, T. Gómez-Acebo, and F. Castro, Continuous and Cyclic Oxidation of T91 Ferritic Steel Under Steam, *Corr. Sci.*, 2004, **46**(3), p 613–631
4. S. Sharafi and M.R. Farhang, Effect of Aluminizing on Surface Microstructure of an HH309 Stainless Steel, *Surf. Coat. Technol.*, 2006, **200**(16–17), p 5048–5051
5. Z.D. Xiang, S.R. Rose, and P.K. Datta, Pack Codeposition of Al and Cr to Form Diffusion Coatings Resistant to High Temperature Oxidation and Corrosion for γ-TiAl, *Mater. Sci. Technol. (UK)*, 2002, **18**(12), p 1479–1484
6. Z.D. Xiang and P.K. Datta, Relationship Between Pack Chemistry and Aluminide Coating Formation for Low-Temperature Aluminisation of Alloy Steels, *Acta Mater.*, 2006, **54**(17), p 4453–4463
7. S.P. Chakraborty, S. Banerjee, K. Singh, I.G. Sharma, A.K. Grover, and A.K. Suri, Studies on the Development of Protective Coating on TZM Alloy and Its Subsequent Characterization, *J. Mater. Process Technol. (Switzerland)*, 2008, **207**(1–3), p 240–247
8. M.T. Kim, N.H. Heo, J.H. Shin, and C.Y. Kim, Simultaneous Chromizing and Aluminizing Using Chromium Oxide and Aluminum: (I) on Low Alloy Steel, *Surf. Coat. Technol.*, 2000, **123**(2–3), p 227–230
9. R. Mevrel, C. Duret, and R. Pichoir, Pack Cementation Processes, *Mater Sci. Technol.*, 1984, **2**(3), p 201–206
10. C.H. Koo and T.H. Yu, Pack Cementation Coatings on Ti_3Al-Nb Alloys to Modify the High-Temperature Oxidation Properties, *Surf. Coat. Technol.*, 2000, **126**(2–3), p 171–180
11. F.J. Pérez, M.P. Hierro, F. Pedraza, M.C. Carpintero, C. Gómez, and R. Tarín, Effect of Fluidized Bed CVD Aluminide Coatings on the Cyclic Oxidation of Austenitic AISI, 304 Stainless Steel, *Surf. Coat. Technol.*, 2001, **145**(13), p 1–7
12. T.L. Hu, H.L. Huang, D. Gan, and T.Y. Lee, The Microstructure of Aluminized Type 310 Stainless Steel, *Surf. Coat. Technol.*, 2006, **201**(6), p 3502–3509
13. F. Üstel and S. Zeytin, Growth Morphology and Phase Analysis of Titanium-Based Coating Produced by Thermochemical Method, *Vacuum.*, 2006, **81**(3), p 360–365
14. R.S. Sundar, R.G. Baligidad, Y.V.R.K. Prasad, and D.H. Sastry, Processing of Iron Aluminides, 1988, *Mater. Sci. Eng. A*, 1998, **258**(1998), p 219–228
15. Y. Mishin and C. Herzig, Diffusion in the Al-Ti System, *Acta Mater.*, 2000, **48**(3), p 589–623
16. M. Entezarian, "Reactive Plasma Spray Forming of Al-$TiAl_3$ Composites Using a Triple Plasma System", Ph.D. Thesis, Department of Minning and Metallurgical Engineering, McGill University, Montreal, Canada, 1997
17. J. Stringer, *Surface Engineering, Series E: Applied Science*, vol. 85, R. Kossowsky and S. Singhal, Ed., 1984, p 561–587
18. M.J. Bennett, A.T. Tuson, C.F. Knights, and C.F. Ayres, Oxidation Protection of Alloy IN 738 LC by Plasma Assisted Vapour Deposited Silica Coating, *Mater. Sci. Technol.*, 1989, **8**, p 841–852
19. R.E. Reed-Hill, *Physical Metallurgy Principles*, 2nd ed., Van Nostrand, New York, 1973